RSC Advances

ROYAL SOCIETY OF CHEMISTRY

www.rsc.org/advances

The dependence of the non-linear creep properties for TATB-based polymer bonded explosives on the molecular structure of polymer binder: (Ⅱ) effects of the comonomer ratio in fluoropolymers

Congmei Lin, Shijun Liu, Zhong Huang, Guansong He, Feiyan Gong, Yonggang Liu, Jiahui Liu *

1,3,5-triamino-2,4,6-trinitrobenzene (TATB) based polymer bonded explosives (PBXs), with three polymer binders containing different molecular structure, were studied by non-linear time dependent creep tests at different temperatures and stresses. Three fluoropolymers, i.e. F2311, F2313, and F2314 with molar ratios of comonomer vinylidene fluoride (VDF) and chlorotrifluoroethylene (CTFE) of 1:1, 1:3, and 1:4 were chosen as polymer binders. The experimental results suggested that all of the materials showed temperature, stress and molecular structure sensitivity. With the decrease of temperature and stress, the creep resistance of three TATB-based PBXs was improved with reduced creep strain, decreased steady-state creep strain rate, and prolonged creep failure time. Replacement of F2311 with F2313 in the binder system leaded to a creep strain decrease and the creep failure time raise. With the further increasing of CTFE content in fluoropolymers from 75% to 80%, the creep resistance performances were enhanced for TATB/F2314 composites under pressures from 1 to 9 MPa, compared with TATB/F2313 composites. The creep strain-time plots for TATB-based PBXs could be accurately fit using the six-element mechanical model. The long-term creep behaviors of TATB-based PBXs were predicted based on time-temperature superposition (TTS) concept. In addition, the dynamic behaviors and mechanical properties of fluoropolymers and TATB-based PBXs were also studied and analyzed in detail.

Key words: applied chemistry TATB polymer bonded explosive molecular structure non-linear creep properties

1. Introduction

Polymer bonded explosives (PBXs) based on explosive crystals and polymer binder are widely used in many defense and industrial fields.[1-3] Generally, PBXs are comprised of 90-95% weight of explosive crystals and 5-10% weight of polymeric binders.[4] It is now well accepted that although the ratio of the polymer binder component is limited to a low value, the component and proportion of polymer binder has a marked influence on the properties of PBX, such as thermal decomposition behaviors, mechanical properties, failure form, aging resistance, and sensitivity.[5-10]

As a typical representative, fluoropolymer is one kind of the most commonly used binders with the advantages of good physical and chemical stability, excellent aging resistance and heat resistance, and great compatibility with other components in composite explosives.[11-15] Several PBX materials have been formulated with fluoropolymer as a binder in the last decades, such as LX-17 (92.5% 1,3,5-triamino-2,4,6-trinitrobenzene TATB and 7.5% fluoropolymer kel-F800 by weight) and PBX-9502 (95% TATB and 5% kel-F800 by weight).[16-18] There are many reports on

Institute of Chemical Materials, China Academy of Engineering Physics, Mianyang, Sichuan 621900, P. R. China. E-mail: huiihuii@163.com; Fax: +86-816-2495856; Tel: +86-816-2482005.

the experiment and simulation study of fluoropolymer and its PBXs. Bourne et al[19] presents experimental data on equation-of-state and shock-induced damage evolution of the fluoropolymer Kel-F800. It is revealed that Kel-F800 shows decreasing spall strength with increasing stress. Gustavsen et al[17] have conducted a series of shock initiation experiments on PBX 9502 cooled to -55 ℃. It is found that wave profiles from embedded gauges are qualitatively similar to those observed at 23 ℃. However, at -55 ℃, PBX 9502 is much less sensitive than at 23 ℃. Zhang et al. [20] have reported the aggregate behaviors of fluoropolymers F2311, F2312, F2313 and F2314 in TATB-based PBX with the dissipative particle dynamics method. The self-aggregate behaviors and the poor wrap property of fluoropolymers in the TATB-based PBX are consistent with the experimental observation. The 'insert' model for β-octahydro-1,3,5,7-tetranitro-1,3,5,7-tetrazocine (HMX)-based PBX has been proposed to study the mechanical properties of HMX/F2311 PBX. It is revealed that the rigidity is weakened and the ductibility is improved by adding a small amount of F2311 in the crystalline HMX.[21] Similar results that the ductility of crystalline TATB can be effectively improved by blending fluorine-containing polymers in small amounts have been found using molecular dynamics simulations.[22]

It is recognized that despite the polymer content being very low, the creep property of the polymer is the main factor in influencing the creep damage properties of PBX.[23] However, few reports have been found with respect to the influences of molecular structure of the polymer binder on the creep performance of PBX.[24,25] In our previous wok, the studies on the effects of the comonomer type of fluoropolymers on the three-point bending creep behaviors of TATB-based PBXs have been conducted.[26] The experimental results show that compared with a copolymer of VDF and CTFE, the incorporation of tetrafluoroethylene and hexafluoropropylene comonomers in fluoropolymer results in a decrease of the steady-state creep strain rate and the maximal creep strain values and an increase of creep rupture time for TATB-based PBXs.

In order to make clear the effects of molecular structure of polymer binder on the non-linear viscoelastic properties of PBX, in this work, creep characterization tests were performed for TATB-based PBXs with three fluoropolymers containing different comonomer ratios (including F2311, F2313, and F2314). Moreover, the dynamic and static mechanical properties and morphologies of the composites were investigated and discussed to understand the relative mechanisms.

2. Experimental Section

2.1 Materials

TATB was supplied by Institute of Chemical Materials, CAEP, China. Three fluoropolymers (F2311, F2313, and F2314) with the molecular structures of -[-(-CF_2-CH_2-)$_a$-(-CF_2-CFCl-)$_b$-]$_n$- were provided by Zhonghao Chenguang Chemical Industry Co., Ltd. China. The molar ratios (a:b) of comonomer vinylidene fluoride (VDF) and chlorotrifluoroethylene (CTFE) in F2311, F2313, and F2314 were 1:1, 1:3, and 1:4, respectively.

2.2 Fabrication of TATB-based PBXs

Three formulations which contained TATB as explosive crystal and copolymer of VDF and CTFE as polymer matrix were designed. TATB-based PBXs with F2311, F2313, and F2314 as polymer binder were labeled as PBX-1, PBX-2, and PBX-3, respectively. The molding powder of TATB-based PBXs was prepared with water suspension methods. Afterwards, the molding powder

product was pressed in a mould and transformed into explosive pellets.

2.3 Characterizations

Dynamic mechanical analysis (DMA) was conducted with a dynamic mechanical analyzer (DMA 242C, NETZSCH, Germany) in a three-point bending mode with specimens' dimensions of 30.0 mm long × 10.0 mm wide × 1.5 mm thick. The tests were performed at 1 Hz with a constant heating rate of 1 ℃/min ranging from -50 to 100 ℃.

All static mechanical properties were examined by a universal testing machine (5582, INSTRON, USA). At least three specimens of each composite were tested, and the average values were reported.

The morphologies and structures of the fracture surface of various TATB-based formulations were identified by a CamScan Apollo 300 (UK) scanning electron microscopy (SEM).

A Netzsch DMA 242C instrument was also used to detect the short-term (less than 5400 s) creep behaviors of various TATB-based PBXs in a three-point bending mode under different temperatures and stresses.

3. Results and Discussion

3.1 Characterization of various fluoropolymers

The viscoelastic properties of the materials, including the information of storage modulus and loss factor (tan delta) of polymers within the measured temperature range could be characterized by dynamic mechanical analysis.[27] Fig. 1 shows the storage modulus and loss factor curves of three fluoropolymers with different VDF/CTFE molar ratios. It is found that the storage modulus of fluoropolymers reduce with increasing temperature. Due to the symmetrical substitution on the quaternary carbon for polyvinylidene fluoride (PVDF), the barrier to internal rotation of polymer main chain is low with good chain flexibility and the glass transition of PVDF is visible at about -30 ℃.[28] Compared with PVDF, the substituent groups are manifolded and the glass transition temperature of polychlorotrifluoroethylene (PCTFE) investigated by Khanna[29] is reported to be 75 ℃. As expected, an improvement in the glass transition temperature of fluoropolymers is also obtained by the decreased VDF/CTFE molar ratio. Consequently, F2311, F2313, and F2314 have the glass transition temperatures of 12.6 ℃, 44.2 ℃, and 55.2 ℃, respectively.

The tensile properties of three fluoropolymers at room temperature have been determined and listed in Table 1. The results indicate that the tensile strength increases with the decrease of VDF/CTFE molar ratio in fluoropolymers. Compared with F2311, the tensile strengthes of F2313 and F2314 are increased by 324.8% and 398.8%.

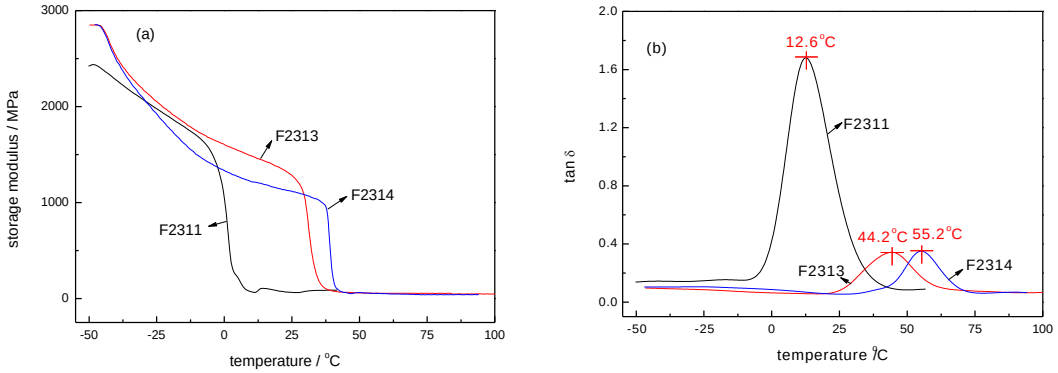

Fig. 1 Dynamic mechanical properties for fluoropolymers with different comonomer ratio: (a) storage modulus (E'), (b) loss factor (tanδ).

Table 1 Tensile properties of three fluoropolymers.

sample	F2311	F2313	F2314
tensile strength / MPa	4.19	17.8	20.9
elongation at break / %	1338.0	325.6	211.0

3.2 Dynamic and static mechanical properties

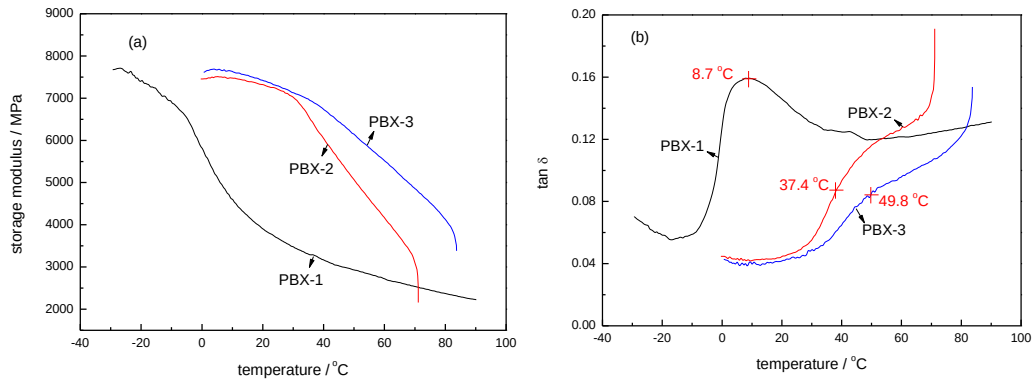

Fig. 2 Dynamic mechanical properties of TATB-based PBXs: (a) storage modulus (E'), (b) loss factor (tanδ).

Dynamic mechanical properties of TATB-based PBXs are reported in Fig. 2. All composites exhibit a decreased storage modulus with increasing temperature. It can be also seen from Fig. 2 that the molecular structure of polymer binder has obvious effects on the PBX's dynamic mechanical properties. The expected improvement in the storage modulus derived from the replacement of F2311 with F2313 and F2314 as polymer matrixs is observed. An inflexion or a peak value, corresponding to the T_g of corresponding polymer binders, exists in the loss factor curves for the TATB-based PBXs. The PBXs becomes soft above this temperature, leading to a sharp drop of storage modulus.

The compressive and tensile mechanical properties were measured using the compressive and Brazilian tests on a circular cylinder 20 mm in diameter by 6-20 mm in height. A description of the method and equipment of Brazilian tests is given elsewhere.[30] Table 2 shows the representative resulting mechanical properties of three TATB-based PBXs at room temperature.

Table 2 Comparison of mechanical properties for three explosives

sample	compressive strength / MPa	compressive elongation at break / %	tensile strength / MPa	tensile elongation at break / %
PBX-1	14.23	3.85	3.20	1.04
PBX-2	24.27	3.09	4.32	0.369
PBX-3	25.81	1.96	4.76	0.143

It can be found from Table 2 that the molecular structure of polymer binder also markedly affects the static mechanical behaviors of the TATB-based PBXs. Compared with PBX-1, a pronounced increase of strength can be noticed for PBX-2 and PBX-3 at room temperature.

3.3 Morphology analysis

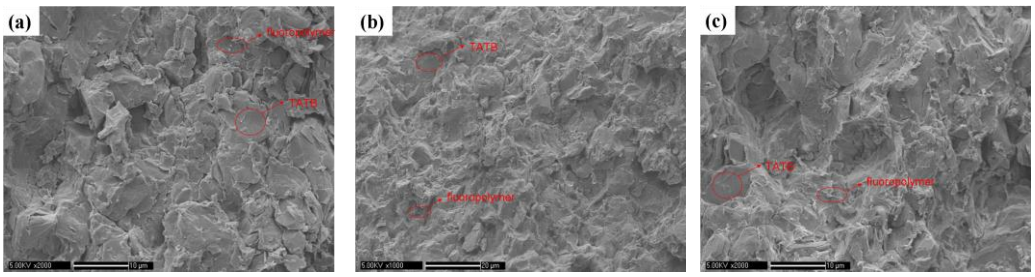

Fig. 3 SEM images of the fracture surface: (a) PBX-1, (b) PBX-2, (c) PBX-3.

The SEM micrographs of the fracture surface for TATB-based PBXs with F2311, F2313, F2314 as polymer binders which are obtained after dynamic mechanical measurements are shown in Fig. 3. It can be clearly seen that filamentous binder exists at the fracture surface of all PBXs, indicating that binder breakage is a kind of the main rupture mode. In addition, the amount of filamentous binder evidently increases with decreasing VDF/CTFE molar ratio.

3.4 Three-point bending creep behaviors of TATB-based PBXs

3.4.1 Stress dependence

The three-point bending creep tests are performed to characterize the creep response of TATB-based PBXs with different fluoropolymers at the stress levels of 1-9 MPa (60 ℃). Fig. 4 shows typical creep data for three samples. The creep performance parameters of TATB-based PBXs, including steady-state creep strain rate, creep failure strain and creep failure time are summarized in Table 3. Clearly, the creep strain of TATB-based PBXs increases with the increase of stress level. The increase of applied stress from 1 MPa to 1.5 MPa of PBX-1 leads to the increase of creep strain in the whole time range. In the case of the more highly loaded material tests (2 MPa), the specimen fractures occur at 705 s. Similar change trends of creep behaviors with stress are also displayed in PBX-2 and PBX-3.

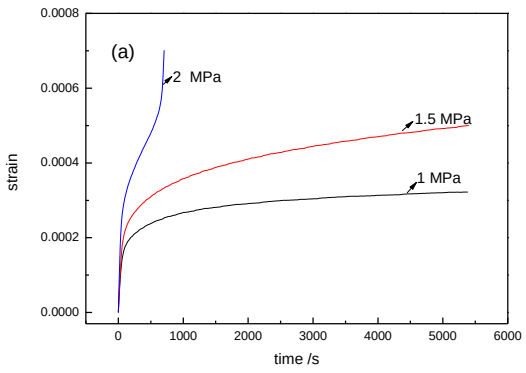

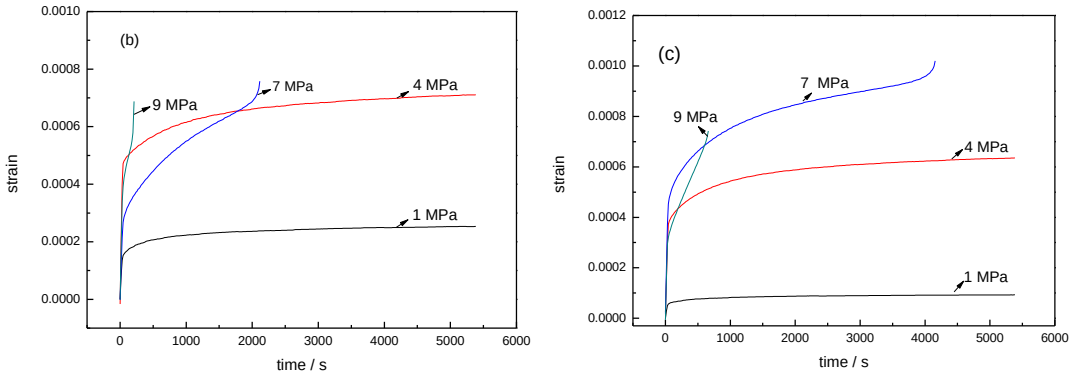

Fig. 4 Stress dependent creep strain of TATB-based PBXs at 60 ℃: (a) PBX-1; (b) PBX-2; (c) PBX-3.

Table 3 The creep performance parameters of TATB-based PBXs under different loading stresses at 60 ℃.

sample	experimental conditions	steady-state creep strain rate / s^{-1}	creep rupture strain	creep rupture time / s
PBX-1	60 ℃/1 MPa	9.237×10^{-9}	$> 3.222\times10^{-4}$	> 5400
	60 ℃/1.5 MPa	2.653×10^{-8}	$> 5.005\times10^{-4}$	> 5400
	60 ℃/2 MPa	3.818×10^{-7}	7.015×10^{-4}	705
PBX-2	60 ℃/1 MPa	5.091×10^{-9}	$> 2.532\times10^{-4}$	> 5400
	60 ℃/4 MPa	1.489×10^{-8}	$> 7.108\times10^{-4}$	> 5400
	60 ℃/7 MPa	1.494×10^{-7}	7.580×10^{-4}	2115
	60 ℃/9 MPa	1.031×10^{-6}	6.879×10^{-4}	210
PBX-3	60 ℃/1 MPa	1.601×10^{-9}	$> 9.274\times10^{-5}$	> 5400
	60 ℃/4 MPa	1.397×10^{-8}	$> 6.356\times10^{-4}$	> 5400
	60 ℃/7 MPa	5.152×10^{-8}	1.020×10^{-3}	4155
	60 ℃/9 MPa	6.022×10^{-7}	7.423×10^{-4}	660

It is evident from Fig. 4 and Table 3 that the molar ratio of comonomer VDF and CTFE in fluoropolymers has a significant impact on the creep response of TATB-based PBXs. The application of F2313 in PBX-2 results in an 44.9% steady-state creep strain rate and 21.4% maximal creep strain at 5400 s decrease as compared to F2311 in PBX-1, when a stress of 1 MPa is used at 60 ℃. As it is shown, no creep fracture occurs up to 7 MPa for PBX-2, while creep fracture occurs at 705 s under 2 MPa for PBX-1. With regard to PBX-3, the application of F2314 binder leads to a further increase of creep resistance. For example, it is found that the steady-state creep strain rate and the creep rupture time of the PBX-3 at 60 ℃/7 MPa are 5.152×10^{-8} s^{-1} and 4155 s. With respect to the composite PBX-2 that contains F2313 binder, the steady-state creep strain rate is reduced by 65.5% and the creep rupture time is increased by 96.5%. Such an obvious rise in creep resistance could be attributed to the higher mechanical strength and glass transition temperature with decreasing VDF/CTFE molar ratio. Compared with F2311, due to the restrained movement of molecular chains in polymer binders F2313 and F2314, the friction between F2313 and F2314 chains is enhanced and thus induces the increased creep resistance of PBX-2 and PBX-3.

3.4.2 Temperature dependence

The constant-stress, three-point bending creep tests are also performed at temperatures ranging

from as low as 30 ℃, up to 80 ℃. In the tests, 1 MPa is carefully selected as the applied stress within the elastic range. The results are displayed in Fig. 5. As expected, the high temperature can bring large creep strain and accelerate the deformation of TATB-based PBXs because of the temperature-activated softening of the polymer matrix.[31] The highest creep strain is observed for PBX-1, which is much higher than that for the PBX-2 and PBX-3 systems at all temperatures.

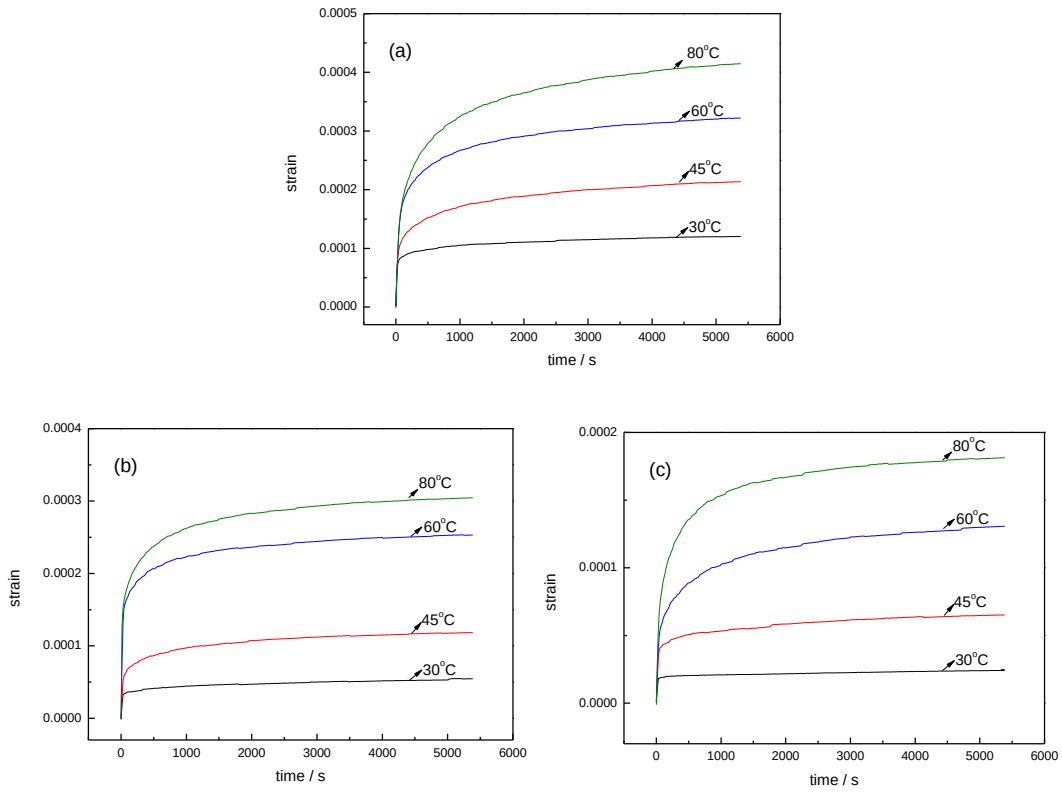

Fig. 5 Temperature dependent creep strain of TATB-based PBXs under 1 MPa: (a) PBX-1; (b) PBX-2; (c) PBX-3.

3.4.3 Creep modeling and analysis

In order to understand the influences of comonomer ratio in fluoropolymers on the creep behaviors of TATB-based PBXs, the six-element mechanical model which is one of the most effective models with high precision is applied in this work. The six-element mechanical model is a combination of a Maxwell element and two Kelvin-Voigt elements.[26] According to the model, the total strain of polymer composite material PBX is the sum of four essentially separate parts and could be determined by:

$$\varepsilon(t) = \varepsilon_1 + \varepsilon_2 + \varepsilon_3 + \varepsilon_4 = \frac{\sigma_0}{E_1} + \frac{\sigma_0}{E_2}\left(1 - e^{-t/\tau_2}\right) + \frac{\sigma_0}{E_3}\left(1 - e^{-t/\tau_3}\right) + \frac{\sigma_0}{\eta_4}t \quad (1)$$

where ε(t) denotes a function of creep strain ε with creep time t, ε_1 is the instantaneous elastic deformation, ε_2 and ε_3 are the high elastic deformation, ε_4 is the viscous flow deformation, σ_0 is the initial stress, E_1 is the elastic modulus of instantaneous elastic deformation, E_2 and E_3 are the elastic modulus of high elastic deformation, τ_2 and τ_3 are the relaxation time, η_4 is the bulk viscosity, respectively.

Fig. 6 shows the experimental and fitting curves of creep behaviors at various temperatures

according to six-element mechanical model, and the six parameters (E_1, E_2, E_3, τ_2, τ_3, and η_4) are defined and summarized in Table 4. It can be clearly seen that the modeling curves show a satisfactory agreement with the experimental data of TATB-based PBXs. Results show that the E_2, E_3, and η_4 of explosives have the same change trend whether for different type explosives or at different temperatures, which indicates they can be used to characterize the creep resistance of explosive material. The increased values of E_2, E_3, and η_4 with decreasing temperature indicate the reinforced mechanical properties of the amorphous regions and increased resistance to viscous flow. Among the modeled six parameters (E_1, E_2, E_3, τ_2, τ_3, and η_4), the parameters E_2 and E_3 seem to increase with decreasing VDF/CTFE molar ratio in fluoropolymers. It can be attributed to the fact that the higher content of CTFE monomers in polymer binder leads to the blockage of molecular thermodynamic movement and an increase of the rigidity of material. In addition, due to the restricted relative slide of molecular chain, the values of η_4 also increase with decreasing VDF/CTFE molar ratio in fluoropolymers.

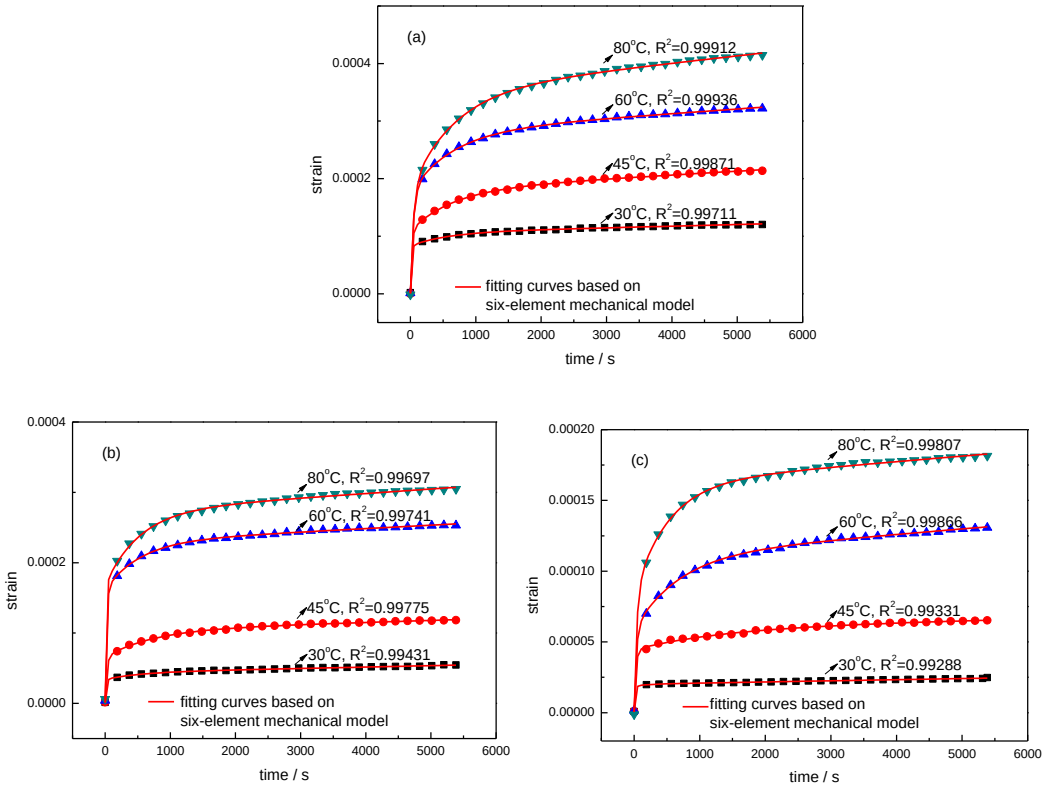

Fig. 6 Modeling results of creep strain curves of TATB-based PBXs under 1 MPa predicted by six-element mechanical model: (a) PBX-1; (b) PBX-2; (c) PBX-3.

Table 4 The simulated parameters of six-element model for TATB-based PBXs under different test conditions.

sample	test condition	E_1 /MPa	E_2 /MPa	τ_2 /s	E_3 /MPa	τ_3 /s	η_4 /MPa s
PBX-1	30 ℃/1MPa	4.394×10^5	4.328×10^4	554.30	1.241×10^4	14.41	3.483×10^8
	45 ℃/1MPa	4.159×10^5	1.429×10^4	651.14	9.312×10^3	23.23	1.505×10^8
	60 ℃/1MPa	1.200×10^7	9.558×10^3	649.35	5.674×10^3	42.99	1.248×10^8
	80 ℃/1MPa	1.129×10^6	5.895×10^3	670.74	5.571×10^3	47.54	7.889×10^7
PBX-2	30 ℃/1MPa	1.176×10^6	1.036×10^5	515.85	3.016×10^4	15.71	5.016×10^8

PBX-3	45 ℃/1MPa	6.690×10^{5}	2.607×10^{4}	739.07	1.557×10^{4}	25.39	3.601×10^{8}
	60 ℃/1MPa	4.376×10^{5}	1.468×10^{4}	526.74	6.297×10^{3}	20.97	2.082×10^{8}
	80 ℃/1MPa	1.300×10^{5}	9.542×10^{3}	525.30	6.234×10^{3}	13.38	1.570×10^{8}
	30 ℃/1MPa	1.859×10^{6}	8.275×10^{5}	243.01	5.439×10^{4}	15.91	1.261×10^{9}
	45 ℃/1MPa	2.468×10^{6}	6.494×10^{4}	1401.03	2.271×10^{4}	25.74	9.222×10^{8}
	60 ℃/1MPa	6.503×10^{6}	1.921×10^{4}	682.68	1.751×10^{4}	32.64	2.604×10^{8}
	80 ℃/1MPa	1.497×10^{6}	1.278×10^{4}	517.99	1.206×10^{4}	38.89	2.565×10^{8}

3.4.4 Prediction of long-term creep behaviors

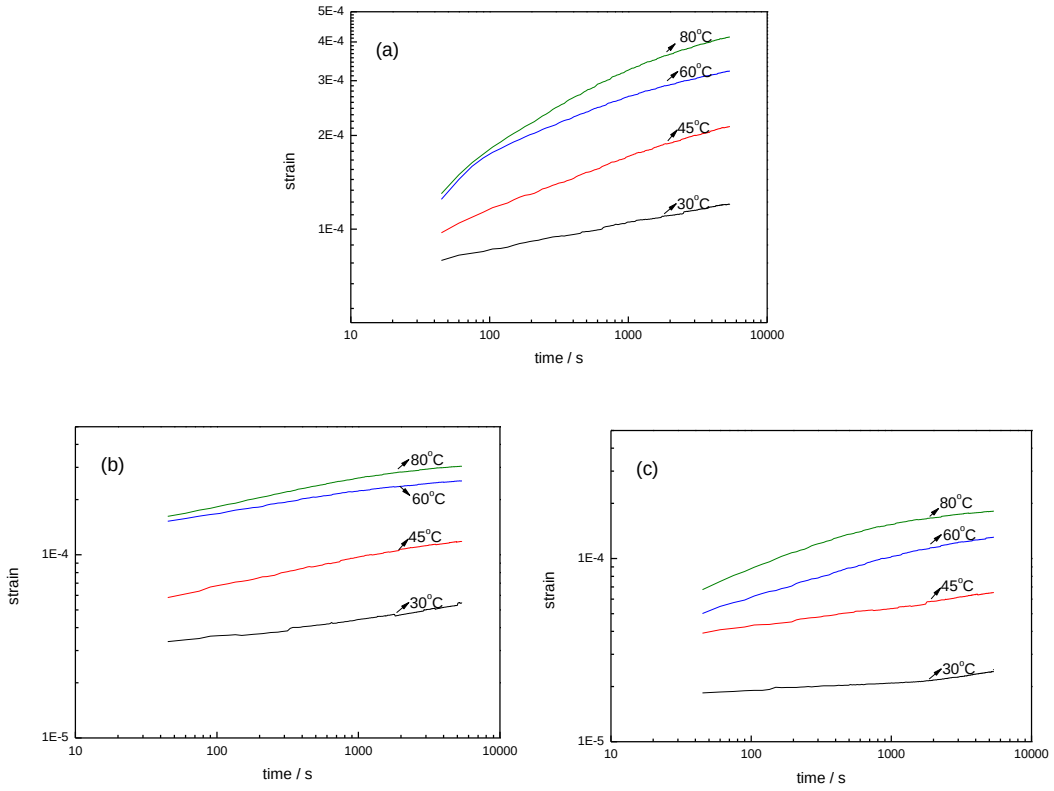

Fig. 7 Double logarithmic plots of three-point bending creep strain for TATB-based PBXs under 1 MPa: : (a) PBX-1; (b) PBX-2; (c) PBX-3.

For the binary TATB/fluoropolymer systems, the creep strains which were measured at a temperature range of 30-80 ℃ (Fig. 5) and a stress of 1 MPa are used to construct the three-point bending master curves of creep strain at the reference temperature of 30 ℃. Fig. 7 gives the representative double logarithmic plots for TATB-based PBXs at different temperatures under 1 MPa. It can be seen that the shape of double logarithmic plots of the individual creep process are similar. Therefore, long-term predictions are easily obtained based on time-temperature superposition (TTS) concept, as presented in Fig. 8. Since the PBX's mechanical properties are dominated by the binder, the master curves of creep strain for PBXs also depend on the molecular structure of polymer binder. The results reveal that the replacement of F2311 by F2313 and F2314 leads to a creep strain decrease within the time scale. The significantly improved creep resistance is due to the mobility restriction of polymer chains with decreasing VDF/CTFE molar ratio.

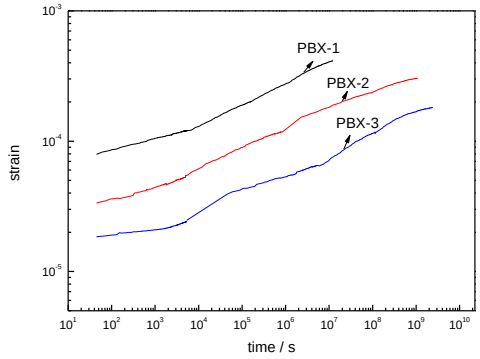

Fig. 8 Three-point bending creep strain master curves of pure TATB and TATB-based PBXs.

4. Conclusions

The present work investigated and compared the creep behaviors of PBXs based on three types of fluoropolymers, i.e. F2311, F2313, and F2314, with different molar ratios of comonomer vinylidene fluoride (VDF) and chlorotrifluoroethylene (CTFE) at various temperatures and stresses. Dynamic mechanical analysis and static mechanical measurement results revealed that the glass transition temperature of fluoropolymer shifted to higher temperatures and the mechanical strength was enhanced with the decrease of VDF/CTFE molar ratio. Consequently, the decrease of VDF/CTFE molar ratio in fluoropolymers remarkably improved the mechanical strength and the creep resistance of TATB-based PBXs. The TATB/F2313 composites showed a significant reduction in the creep deformation and a dramatically increase in the creep failure time, compared to that of the TATB/F2311 composites. The improved creep properties of the composites were likely attributed to the inhibited mobility of F2313 molecular chains. The molar ratio of comonomer VDF and CTFE for polymer binder change from 1:3 (F2313) to 1:4 (F2314) results in a further modification of creep behaviors. Based on the analytical modeling (six-element mechanical model) and experimental results, the influences of molecular structure of polymer binder on the creep performance of TATB-based PBXs were discussed. The long-term creep behavior, which was predicted based on time-temperature superposition (TTS) concept, suggested that the TATB/F2314 composites provided much lower creep response compared to that of the TATB/F2311 and TATB/F2313 composites. The research presented here indicated that changing the molecular structure in polymer binder, such as comonomer molar ratio, is an effective way to tune the creep performance of the PBXs.

References

1 S. F. Trevino, and D. A.Wiegand, *J. Energ. Mater.*, 2008, **26**, 79-80.

2 A. Wuillaume, A. Beaucamp, F. David-Quillot and C. Eradès, *Propell. Explos. Pyrot.*, 2014, **39**, 390-396.

3 Q. Yan, S. Zeman, and A. Elbeih, *Thermochim. Acta*, 2012, **537**, 1-12.

4 P. W. Cooper and S. R. Kurowski, Introduction to the Technology of Explosives, New York: Wiley-VCH, p.21-23, 1996.

5 S. F. Trevino and D. A. Wiegand, *J. Energ. Mater.*, 2008, **26**, 79-80.

6 C. M. Tarver and J. G. Koerner, *J. Energ. Mater.*, 2008, **26**, 1-28.

7 D. M. Hoffman, *J. Energ. Mater.*, 2001, **19**, 163 - 193.

8 H. F. Rizzo, J. R. Humphrey, and J. R. Kolb. Growth of 1,3,5-triamino-2,4,6-trinitrobenzene (TATB). Ⅱ.Control of growth by use of high Tg polymeric bingers, *Propell. Explos. Pyrot.*, 1981, **6**, 27-36..

9 J. Xiao, X. Ma, W. Zhu, Y. Huang, H. Xiao, H. Huang, and J. Li, *Propell. Explos. Pyrot.*, 2007, **32**, 355-359.

10 X. Ma, J. Xiao, H. Huang, X. Ju, J. Li, and H. Xiao, *Chinese J. Chemi*., 2006, **24**, 473-477.

11 L. L. Stevens, D. M. Dattelbaum, M. Ahart, and R. J. Hemley, *J. Appl. Phys.*, 2012, **112**, 023523.

12 Q. L. Yan, S. Zeman, and A. Elbeih, *Thermochim. Acta*, 2013, **562**, 56-64.

13 C. Lin, J. Liu, G. He, L. Chen, Z. Huang, F. Gong, Y. Liu, S. Liu, *RSC Adv.*, 2015, **5**, 35811-35820.

14 C. Lin, J. Liu, S. Liu, X. Tu, Z. Huang, Y. Li, and J. Zhang, *Chinese J. Energ. Mater.*, 2014, **22**, 798-803.

15 D. M. Hoffman, *Polym. Eng. Sci.*, 2003, **43**, 139-156.

16 C. Souers, P. Lewis, M. Hoffman, and B. Cunningham, *Propell. Explos. Pyrot.*, 2011, **36**, 335-340.

17 R. L. Gustavsen, R. J. Gehr, S. M. Bucholtz, R. R. Alcon, and B. D. Bartram, *J. Appl. Phys.*, 2012, **112**, 074909.

18 W. Small IV, E. A. Glascoe, and G. E. Overturf, *Thermochim. Acta*, 2012, **545**, 90-95.

19 N. K. Bourne and G. T. Gray III, *J. Appl. Phys.*, 2005, **98**, 123503.

20 Y. Zhang, G. Ji, F. Zhao, Z. Gong, D. Wei, L. Chen, and W. Li, *Mol. Simulat.*, 2011, **37**, 237-242.

21 J. Xiao, W. Zhu, X. Ma, H. Xiao, H. Huang, and J. Li, *Mol. Simulat.*, 2008, **34**, 775-779.

22 J. Xiao, X. Ma, W. Zhu, Y. Huang, H. Xiao, H. Huang, and J. Li, *Propell. Explos. Pyrot.*, 2007, **32**, 355-359.

23 Y. Ding, Y. Pan, R. Cai, X. Yu, and Y. Yang, *Chinese J. Energ. Mater.*, 2000, **8**, 87-90.

24 C. Lin, S. Liu, X. Tu; Z. Huang, Y. Li, L. Pan, and J. Zhang, *Propell. Explos. Pyrot.*, DOI: 10.1002/prep.201400203.

25 C. Lin, J. Liu, F. Gong, G. Zeng, Z. Huang, L. Pan, J. Zhang, and S. Liu, *RSC Adv.*, 2015, **5**, 21376-21383.

26 C. Lin, S. Liu, Z. Huang, G. He, F. Gong, Y. Liu, and J. Liu, *RSC Adv.*, 2015, **5**, 30592-30601.

27 X. Wang, L. Gong, L. Tang, K. Peng, Y. Pei, L. Zhao, Lian-Bin Wu, and J. Jiang, *Compos. Part A: Appl. Sci. Manuf.*, 2015, **69**, 288-298.

28 P. Frübing, F. Wang, and M. Wegener, *Appl. Phys. A: Mater. Sci. Process.*, 2012, **107**, 603-611.

29 Y. P. Khanna and R. Kumar, *Polymer*, 1991, **32**, 2010-2013.

30 M. Wen, W. Tang, X. Zhou, H. Pang, and F. Zhu, *Chinese J. Energ. Mater.*, 2013, **21**, 490-494.

31 M. Ganss, B. K. Satapathy, M. Thunga, R. Weidisch, P. Potschke, and A. Janke. *Macromol. Rapid Commun*. 2007, **28**, 1624-1633.